State-space identification of switching linear discrete time-periodic systems with known scheduling signals

İsmail UYANIK[1,2,*] ◎, **Hasan HAMZAÇEBİ**[3] ◎, **M. Mert ANKARALI**[4] ◎

[1]Laboratory of Computational Sensing and Robotics, Johns Hopkins University, Baltimore, MD, USA
[2]Department of Electrical and Electronics Engineering, Hacettepe University, Ankara, Turkey
[3]Microelectronics, Guidance, and Electro-Optics Business Sector, ASELSAN Inc., Ankara, Turkey
[4]Department of Electrical and Electronics Engineering, Middle East Technical University, Ankara, Turkey

Abstract: In this paper, we propose a novel frequency domain state-space identification method for switching linear discrete time-periodic (LDTP) systems with known scheduling signals. The state-space identification problem of linear time-invariant (LTI) systems has been widely studied both in the time and frequency domains. Indeed, there have been several studies that also concentrated on state-space identification of both continuous and discrete linear time-periodic (LTP) systems. The focus in this study is the family of LDTP systems that switch among a finite set of subsystems triggered by known periodic scheduling signals. We address the state-space identification of such systems in frequency domain using input–output data. We also assume that full state measurements are available for the identification process. The major difference of our study is that we explicitly model the known scheduling signals responsible for switching, which greatly reduces the parametric complexity as well as potentially increases the estimation accuracy by avoiding overfitting. In our identification framework, we gather the Fourier transformations of input–output data, known periodic scheduling signals, and state-space system dimensions and fuse them in a linear regression framework. Later, we estimate the Fourier series coefficients of the time-periodic system and input matrices using a least-squares solution. Finally, we illustrate the effectiveness of our method using a switching LDTP system that is based on the damped Mathieu equation.

Key words: Linear time periodic systems, system identification, state-space identification, switching systems

1. Introduction

This paper focuses on frequency-domain state-space identification of "hybrid" linear discrete-time periodic (LDTP) systems. The class of LDTP systems we are interested in here includes a finite number of switching subsystems that are alternated based on a periodic scheduling signal. Usually in the literature, such scheduling signals are assumed to be known or can be accurately measured in real-time [1–5]. We also stick to the same assumption and assume full state measurement of the underlying dynamical system. However, on the contrary, we use a more general subsystem formulation (to make it applicable for legged locomotion problems [6]), where our subsystem dynamics can also be time-periodic, different than most of the recent studies on this topic, which focused on time-invariant subsystem dynamics [2, 7].

The class of systems we consider appears in a wide range of dynamical phenomena from biology to engineering, such as legged locomotion [6, 8], helicopter rotor dynamics [9], inverter locomotives [10], and wind turbines [11]. Initial formulations of this type of systems are generally modeled as nonlinear hybrid dynamical

---

*Correspondence: uyanik@jhu.edu

systems that include some state-dependent scheduling functions [12–15]. However, a vast majority of the system identification studies for such systems focus on their local behavior around a periodic orbit. Hence, linearization of such nonlinear hybrid dynamics around a limit cycle yields a linear time-periodic (LTP) system, where the state-dependent switching functions can also be approximated as time- or phase-dependent periodic scheduling signals [12, 16, 17].

The fact that an LTP system can be lifted to a multiinput multioutput linear time-invariant (LTI) system equivalent allows using LTI system identification tools (with some extensions) for LTP systems as well [18–20]. However, the hybrid nature of the class of systems we are interested in introduces "instant jumps" between different vector fields and is thus open to developing new tools that explicitly take the time-dependent (and possibly nonsmooth) changes in system dynamics into account. In time domain analysis, such periodic scheduling functions can be simply modeled as rectangular wave functions. However, in frequency domain analysis, the effect of such signals (if not separated from the underlying system dynamics) may spread over all frequencies and contaminate the frequency response functions [17]. Therefore, a careful characterization of such periodic scheduling functions becomes important to identify underlying system dynamics.

In our previous work, we proposed a similar system identification method for a class of hybrid linear continuous time-periodic systems [4]. Here, in this study our goal is to develop a similar methodology for hybrid linear discrete time-periodic systems. Indeed, discrete-time formulation leads us to cover a much broader class of systems due to the fact that discrete time instants associated with the system formulation does need to be synchronized with actual "time" and they can be associated with special events triggered by state-dependent threshold functions [12]. For example, in a hybrid dynamical system that operates around an isolated limit-cycle, one can choose a set of selected discrete phase coordinates (i.e. set of Poincaré sections) as "time-instants", which can even include the hybrid-transition events.

In this context, we propose a new state-space identification method for LDTP systems with known scheduling signals. In Section 2, we establish the problem formulation. Then, in Section 3, we present the proposed system identification methodology. We provide an illustrative numerical example in Section 4 and provide the concluding remarks in Section 5.

2. Problem formulation

The stable, linear discrete time-periodic systems we are interested in have the state-space form

$$
\begin{aligned}
x_{k+1} &= A_k x_k + B_k u_k \ , \\
y_k &= C x_k \ ,
\end{aligned}
\tag{1}
$$

where $A_k \in \mathbb{R}^{m \times m}$, $B_k \in \mathbb{R}^{m \times 1}$ and $C = I^{m \times m}$ such that I is the $m \times m$ identity matrix. The system and input matrices (A_k and B_k) are time-periodic with a common system period N (yielding a periodic frequency of $\omega_0 = 2\pi/N$) where $A_k = A_{k+pN}$ and $B_k = B_{k+pN}$ for $\forall p \in \mathbb{Z}$. We call the class of systems in the form of Eq. (1) $\Upsilon(A_k, B_k)$.

The class of the systems defined by $\Upsilon(A_k, B_k)$ that we are interested in has hybrid dynamics that originate from the switching nature of the system and input matrices based on a known periodic scheduling signal. Hence, the system and input matrices can be written as

$$
A_k = \sum_{i=1}^{M} A_k^i s_k^i \ , \quad B_k = \sum_{i=1}^{M} B_k^i s_k^i,
\tag{2}
$$
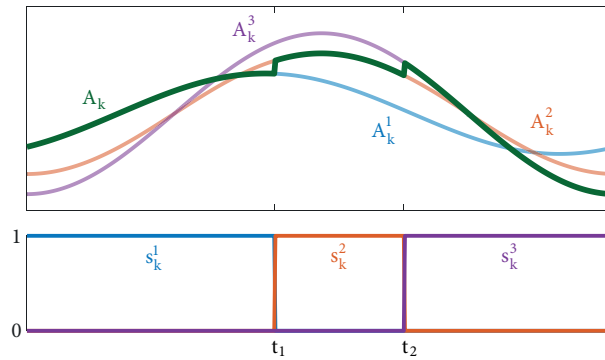
Figure 1. A sample illustration for a scalar switching system with time-periodic subsystem dynamics. Green line shows the resulting dynamics, A_k, obtained by the combination of three subdynamics, A_k^1, A_k^2, and A_k^3, which are activated by s_k^1, s_k^2, and s_k^3, respectively.

where A_k^i and B_k^i correspond to ith time-periodic subsystem matrices that are activated by the corresponding scheduling function, s_k^i. Note that one of the key differences of our problem statement is that our modeling considers all subsystem dynamics to be time-periodic as well rather than assuming time-invariant subsystem dynamics as seen in a majority of the studies in the literature [2, 7, 21, 22].

Assumption 1 *The "known" periodic scheduling signals, s_k^i for $i = 1, 2, \cdots, M$, are rectangular wave functions ensuring that only one of the subdynamics pair (A_k^i, B_k^i) is active for any time instant. Besides, active durations of these signals span the entire system period ensuring that one subdynamics pair (A_k^i, B_k^i) is active at any time instant (see Figure 1 for an illustration).* □

Given the definitions above, the problem that we are interested in here can be stated as below.

Problem 1 *Estimate a state-space model $\Upsilon(\hat{A}_k, \hat{B}_k)$ for Eq. (1) to obtain an input–output equivalent system model (see Remark 1) given*

- *input–output data pairs, where the inputs, u_k^i, are different frequency single-sine signals and the outputs, x_k^i, are the corresponding state measurements, and*

- *the periodic scheduling signals, s_k^i, for $i = 1, 2, \cdots, M$ and hence the system period, N.* □

Remark 1 *Note that in standard state-space identification methods, such as the subspace identification methods, the estimated system can be found only up to a similarity transformation [23–25]. However, since we assume full state measurement, we limit the output matrix to being an identity matrix. Hence, the proposed method yields an approximate estimation for the original state-space model parameters, leaving no other possibility for a similarity transformation.* □

3. Identification of state-space structure

Our analysis starts by taking the Fourier series expansion of the time-periodic system and input matrices in Eq. (1) as

$$A_k = \sum_{n=-N/2}^{N/2-1} \mathcal{A}_n e^{j2\pi nk/N} , \quad B_k = \sum_{n=-N/2}^{N/2-1} \mathcal{B}_n e^{j2\pi nk/N}, \tag{3}$$

where $\mathcal{A}_n$ and $\mathcal{B}_n$ are discrete Fourier series coefficients for A_k and B_k, respectively. Note that DFT results in a finite number of Fourier series coefficients, which are also periodic with N, meaning that

$$\mathcal{A}_n = \mathcal{A}_{n+pN}, \forall p \in \mathbb{Z}, \tag{4}$$

where the same expression is also valid for $\mathcal{B}_n$.

Plugging Eq. (3) into the state equation of Eq. (1) yields

$$x_{k+1} = \sum_{n=-N/2}^{N/2-1} \mathcal{A}_n e^{j2\pi nk/N} x_k + \sum_{n=-N/2}^{N/2-1} \mathcal{B}_n e^{j2\pi nk/N} u_k . \tag{5}$$

At steady state, discrete Fourier transform (DFT) of Eq. (5) yields

$$e^{j2\pi n/N} X_n = \sum_{l=-N/2}^{N/2-1} \mathcal{A}_l X_{n-l} + \sum_{l=-N/2}^{N/2-1} \mathcal{B}_l U_{n-l} , \tag{6}$$

where X_n and U_n are discrete Fourier series coefficients for the time-periodic state and input signals, x_k and u_k, respectively.

Fact 1 *[26] Let f_k^1 and f_k^2 be two time-periodic signals, which are both periodic with a common period, K. Let f_k be*

$$f_k = f_k^1 f_k^2. \tag{7}$$

Then the discrete Fourier series coefficients, $\mathcal{F}_n$, of f_k can be obtained as

$$\mathcal{F}_n = \sum_{q=-K/2}^{K/2-1} \mathcal{F}_q^1 \mathcal{F}_{n-q}^2 , \tag{8}$$

where $\mathcal{F}_n^1$ and $\mathcal{F}_n^2$ are the discrete Fourier series coefficients of f_k^1 and f_k^2, respectively. □

Corollary 1 *By Fact 1, the discrete Fourier series coefficients, $\mathcal{A}_n$ and $\mathcal{B}_n$, of the time-periodic system and input matrices A_k and B_k can be written as*

$$\mathcal{A}_n = \sum_{i=1}^{M} \sum_{q=-N/2}^{N/2-1} \mathcal{A}_q^i S_{n-q}^i ,$$

$$\mathcal{B}_n = \sum_{i=1}^{M} \sum_{q=-N/2}^{N/2-1} \mathcal{B}_q^i S_{n-q}^i , \tag{9}$$

where $\mathcal{A}_q^i$ and $\mathcal{B}_q^i$ are the discrete Fourier series coefficients of the ith subsystem system and input matrices A_k^i and B_k^i, respectively. Also, S_n^i corresponds to the discrete Fourier series coefficients of the ith periodic scheduling signal. $\qquad\qquad\square$

Now, substituting Eq. (9) into Eq. (6) yields

$$e^{j2\pi n/N}X_n = \sum_{l=-N/2}^{N/2-1}\sum_{i=1}^{M}\sum_{q=-N/2}^{N/2-1}\mathcal{A}_q^i S_{l-q}^i X_{n-l} + \sum_{l=-N/2}^{N/2-1}\sum_{i=1}^{M}\sum_{q=-N/2}^{N/2-1}\mathcal{B}_q^i S_{l-q}^i U_{n-l} \ . \tag{10}$$

Note that $\mathcal{A}_q^i$ and $\mathcal{B}_q^i$ for $i=1,2,\ldots,M$ and $q=-N/2,\ldots,N/2-1$ are the only unknown terms in Eq. (10).

For the sake of our analysis, we reorganize the terms in Eq. (10) such that the "known" terms can be isolated from the unknowns as

$$e^{j2\pi n/N}X_n = \sum_{i=1}^{M}\sum_{q=-N/2}^{N/2-1}\mathcal{A}_q^i\left\{\sum_{l=-N/2}^{N/2-1}S_{l-q}^i X_{n-l}\right\} + \sum_{i=1}^{M}\sum_{q=-N/2}^{N/2-1}\mathcal{B}_q^i\left\{\sum_{l=-N/2}^{N/2-1}S_{l-q}^i U_{n-l}\right\} \ . \tag{11}$$

The terms inside the brackets of Eq. (11) are all "known" and measured components. Thus, we define two new variables and perform some change of indices to represent these terms as

$$\begin{aligned}
\mathbf{X}_{n-q}^i &:= \sum_{l=-N/2}^{N/2-1}S_{l-q}^i X_{n-l} = \sum_{r=-N/2}^{N/2-1}S_r^i X_{n-q-r} \ , \\
\mathbf{U}_{n-q}^i &:= \sum_{l=-N/2}^{N/2-1}S_{l-q}^i U_{n-l} = \sum_{r=-N/2}^{N/2-1}S_r^i U_{n-q-r} \ ,
\end{aligned} \tag{12}$$

for $i=1,2,\ldots,M$. Hence, Eq. (11) can be simplified as

$$e^{j2\pi n/N}X_n = \sum_{i=1}^{M}\sum_{q=-N/2}^{N/2-1}\mathcal{A}_q^i\mathbf{X}_{n-q}^i + \sum_{i=1}^{M}\sum_{q=-N/2}^{N/2-1}\mathcal{B}_q^i\mathbf{U}_{n-q}^i \ . \tag{13}$$

The goal of our analysis is to transform Eq. (13) into a linear regression form, such that we can solve for the unknowns using basic least squares analysis. Note that Eq. (13) includes known and unknown terms in both summations. To overcome this issue, we utilize a matrix multiplication formulation by combining the known and unknown terms in matrices as follows (see Remark 2):

$$\begin{aligned}
\bar{\mathcal{A}}^i &:= [\mathcal{A}_{-N/2}^i \ldots \mathcal{A}_0^i \ldots \mathcal{A}_{N/2-1}^i], \\
\bar{\mathcal{B}}^i &:= [\mathcal{B}_{-N/2}^i \ldots \mathcal{B}_0^i \ldots \mathcal{B}_{N/2-1}^i], \\
\mathbf{X}_n^i &:= [\mathbf{X}_{n+N/2}^i \ldots \mathbf{X}_n^i \ldots \mathbf{X}_{n-(N/2-1)}^i]^T, \\
\mathbf{U}_n^i &:= [\mathbf{U}_{n+N/2}^i \ldots \mathbf{U}_n^i \ldots \mathbf{U}_{n-(N/2-1)}^i]^T.
\end{aligned} \tag{14}$$

Remark 2 *Different than continuous-time LTP system identification methods (as in [4]), the Fourier series coefficients of the linear discrete time-periodic (LDTP) systems are finite. Hence, our solution methodology for*

LDTP systems does not require a truncation for the Fourier series coefficients that will be considered for system identification at this step. □

Having the new variables defined in Eq. (14), we can now transform Eq. (13) to a simpler form as

$$e^{j2\pi n/N}X_n = \sum_{i=1}^{M} \bar{\mathcal{A}}^i \mathbf{X}_n^i + \sum_{i=1}^{M} \bar{\mathcal{B}}^i \mathbf{U}_n^i \;. \tag{15}$$

An important point that needs to be resolved at this step is that the estimated time-domain state-space model, $\Upsilon(\hat{A}_k, \hat{B}_k)$, should be real-valued. This requires the estimated Fourier series coefficients to be in complex conjugate form. To avoid any numerical issues regarding this problem, we aim to enforce our estimates for the Fourier series coefficients to be in complex conjugate form at this step. Note that the matrices in Eq. (14) contain complex conjugate numbers, except the 0th and $(-N/2)$th terms, which should already be real-valued by the definition of discrete Fourier transform. We define a right-hand-side transformation matrix, $P_{(N,m)}$, which separates the real and imaginary parts of the complex conjugate numbers without changing the dimension as

$$P_{(N,m)} := \begin{bmatrix} \mathcal{I}_m & 0 & 0 & 0 \\ 0 & \mathcal{I}_{(N/2-1)m} & 0 & j\mathcal{J}_{(N/2-1)m} \\ 0 & 0 & \mathcal{I}_m & 0 \\ 0 & \mathcal{J}_{(N/2-1)m} & 0 & -j\mathcal{I}_{(N/2-1)m} \end{bmatrix} , \tag{16}$$

where $\mathcal{I}_q$ is a $q \times q$ identity matrix while $\mathcal{J}_q$ is a $q \times q$ antidiagonal identity matrix. By using Eq. (16), $\bar{\mathcal{A}}^i$ and $\bar{\mathcal{B}}^i$ in Eq. (15) can be rewritten as

$$\begin{aligned} \widetilde{\mathcal{A}}^i &:= \bar{\mathcal{A}}^i P_{(N,m)} \;, \\ \widetilde{\mathcal{B}}^i &:= \bar{\mathcal{B}}^i P_{(N,1)} \;. \end{aligned} \tag{17}$$

Now, by using the new variables defined in Eqs. (16) and (17), we obtain a simpler form for Eq. (15) as

$$e^{j2\pi n/N}X_n = \sum_{i=1}^{M} \widetilde{\mathcal{A}}^i P_{(N,m)}^{-1} \mathbf{X}_n^i + \sum_{i=1}^{M} \widetilde{\mathcal{B}}^i P_{(N,1)}^{-1} \mathbf{U}_n^i \;. \tag{18}$$

At this step, we can transform Eq. (18) to matrix algebra by combining the known and unknown terms in different matrices as

$$\begin{aligned} \kappa^T &:= [\widetilde{\mathcal{A}}^1 \dots \widetilde{\mathcal{A}}^M \;\; \widetilde{\mathcal{B}}^1 \dots \widetilde{\mathcal{B}}^M] \;, \\ \gamma_n^T &:= \mathcal{P}^{-1}[\mathbf{X}_n^1 \dots \mathbf{X}_n^M \;\; \mathbf{U}_n^1 \dots \mathbf{U}_n^M]^T \;, \end{aligned} \tag{19}$$

where $\mathcal{P}^{-1}$ is a matrix that includes M of $P_{(N,m)}^{-1}$ and M of $P_{(N,1)}^{-1}$ in its diagonals. Thus, Eq. (18) can be simplified to

$$\widetilde{y}_n = \gamma_n \kappa, \tag{20}$$

where $\widetilde{y}_n^T = e^{j2\pi n/N}X_n$.

As explained before, one of the key properties of LDTP systems is that when a sinusoidal input signal is given to an LDTP system, the output will not be only at the input frequency (as in the case of LTI systems) but also in the harmonics of the pumping frequency of the system. Therefore, one needs to evaluate Eq. (20) for all of these harmonic responses in order to consider the effect of harmonics during the system identification process. Therefore, our solution methodology includes evaluating Eq. (20) in all of the harmonic response frequencies for a more accurate characterization of the LDTP system dynamics. Let the LTP system we are interested in have a maximum of H harmonic responses across the frequency range that we are interested in for the system identification. We can now evaluate Eq. (20) for each of these harmonic frequencies by performing a circular shift operation. The resulting data matrices hence take the following form:

$$
\Gamma_{\omega_i} = \begin{bmatrix} \gamma_{-N/2} \\ \vdots \\ \gamma_0 \\ \vdots \\ \gamma_{N/2-1} \end{bmatrix} , \ Y_{\omega_i} = \begin{bmatrix} \widetilde{y}_{-N/2} \\ \vdots \\ \widetilde{y}_0 \\ \vdots \\ \widetilde{y}_{N/2-1} \end{bmatrix} , \tag{21}
$$

which yields the following equation:

$$
\Gamma_{\omega_i} \kappa = Y_{\omega_i} . \tag{22}
$$

Note that Eq. (22) considers data only from a single input frequency. One of the advantages of working with frequency domain data is the ability to simply combine data from multiple experiments. Hence, we combine frequency response data from multiple input frequencies as

$$
\underbrace{\begin{bmatrix} \vdots \\ \Gamma_{\omega_i} \\ \vdots \end{bmatrix}}_{\bar{\Gamma}} \kappa = \underbrace{\begin{bmatrix} \vdots \\ Y_{\omega_i} \\ \vdots \end{bmatrix}}_{\bar{\mathcal{Y}}} , \tag{23}
$$

where K is the number of different frequency input signals. Finally, to achieve real-valued solutions for κ, we separate the real and imaginary parts of Eq. (23) as

$$
\underbrace{\begin{bmatrix} Re\{\bar{\Gamma}\} \\ Im\{\bar{\Gamma}\} \end{bmatrix}}_{\Gamma} \kappa = \underbrace{\begin{bmatrix} Re\{\bar{\mathcal{Y}}\} \\ Im\{\bar{\mathcal{Y}}\} \end{bmatrix}}_{\mathcal{Y}} . \tag{24}
$$

The solution for κ of Eq. (24) can be simply found by using a least square solution when $\Gamma^H \Gamma$ is invertible (see Remark 3).

Remark 3 *The invertibility of $\Gamma^H \Gamma$ depends on many factors such as the number of switching subsystems, the duty factor of each scheduling signal, and the frequency components of the switching subsystems. Thus, it is not possible to provide a general invertibility criterion without constraining the problem definition at this step. To avoid this, the theoretical investigation of invertibility requirements is left out of the scope of the current paper. However, we utilize a computational method by reducing the number of harmonic responses that will be considered for Eq. (14) to ensure analytical least squares solutions as described below.*

Note that the formulation for κ given in Eq. (19) includes N unknown Fourier series coefficients for each system and input matrices. However, we assume that the internal switching subsystems are respectively smooth time-periodic functions and the number of unknown Fourier series coefficients is limited. Note that this assumption does not limit the number of harmonics N that can be observed in the resulting switching system $(A_k,\ B_k)$ due to the rectangular wave-type scheduling signals. Our assumption only limits the number of unknown Fourier series coefficients of each switching subsystem, $(A_k^i,\ B_k^i)$. This is a fair assumption when the switching subsystems are smooth but the resultant system includes many harmonic components (such as in the case of legged locomotion [27]). Thus, we limit the number of Fourier series coefficients for each subsystem, $(A_k^i,\ B_k^i)$, to the lowest H frequencies in Eq. (14). For example, the truncated unknown Fourier series coefficients vectors, which will replace the ones in Eq. (19), for $(A_k^i,\ B_k^i)$ can now be written as

$$
\begin{aligned}
\bar{\mathcal{A}}^{\dagger i} &:= [\mathcal{A}_{-H}^i \dots \mathcal{A}_0^i \dots \mathcal{A}_H^i], \\
\bar{\mathcal{B}}^{\dagger i} &:= [\mathcal{B}_{-H}^i \dots \mathcal{B}_0^i \dots \mathcal{B}_H^i].
\end{aligned}
\tag{25}
$$

Revising the associated equations, Eqs. (15)–(24), with the truncated form of $\bar{\mathcal{A}}^{\dagger i}$ and $\bar{\mathcal{B}}^{\dagger i}$ yields

$$
\Gamma^{\dagger}\kappa^{\dagger} = \mathcal{Y}\,,
\tag{26}
$$

which can be solved by using a least square solution as

$$
\hat{\kappa}^{\dagger} = (\Gamma^{\dagger H}\Gamma^{\dagger})^{-1}\Gamma^{\dagger H}\mathcal{Y}.
\tag{27}
$$

At this point, one can compute an estimate for the original time periodic system by back-substituting $\hat{\kappa}^{\dagger}$ into Eqs. (25), (19), (17), (14), (9), and (3).

Remark 4 *Note that continuous-time LTP systems can be transformed to discrete-time equivalents by bilinear (Tustin) transformation (see [17] for a special derivation). Hence, the proposed technique can also be utilized for continuous-time LTP systems by sampling the input–output data of the original unknown continuous-time LTP system. Then the estimated discrete-time LTP system can be transformed back to the continuous-time version via inverse bilinear (Tustin) transformation.*

4. Numerical example: a switching piecewise smooth LDTP system

In this section, we present an example simulation study in order to evaluate the performance of the proposed algorithm. To achieve this, we worked on a hybrid damped Mathieu equation form that has piecewise smooth switching system dynamics. The Mathieu equation has been widely used in the literature to model various phenomena such as stability analysis of floating bodies [28], vibrations in elliptic drums [29], and the analysis of radio frequency quadruple [30]. Thus, Mathieu equations may serve as a model for many real-world applications [31].

The piecewise smooth N-periodic LDTP system example we use in this section can be written as a difference equation with time-varying coefficients as

$$
x_{k+2} - \underbrace{\beta(\zeta - \sin(\omega_0 k/N))}_{\xi_k}\,x_{k+1} - \underbrace{\beta(\zeta + \cos(\omega_0 k/N))}_{\mu_k}\,x_k = u_k,
\tag{28}
$$

where μ_k and ξ_k represent piecewise smooth compliance and damping coefficients, respectively. The piecewise hybrid nature of these parameters originate from a known scheduling signal, which switches the parameters β and ζ periodically. Equations of motion for the resulting switching LDTP system structure can be written as

$$x_{k+2} = \begin{cases} \xi_k^1 x_{k+1} + \mu_k^1 x_k + u_k , & \text{if } zN \le k < zN + N/2 , \forall z \in Z \\ \xi_k^2 x_{k+1} + \mu_k^2 x_k + u_k , & \text{if } zN + N/2 \le k < (z+1)N. \end{cases} \tag{29}$$

This difference equation can also be transformed to the state-space form of Eq. (1) for a more intuitional representation as

$$A_k^1 = \begin{bmatrix} 0 & 1 \\ \beta_1(\zeta_1 + \cos(\omega_0 k/N)) & \beta_1(\zeta_1 - \sin(\omega_0 k/N)) \end{bmatrix},$$

$$A_k^2 = \begin{bmatrix} 0 & 1 \\ \beta_2(\zeta_2 + \cos(\omega_0 k/N)) & \beta_2(\zeta_2 - \sin(\omega_0 k/N)) \end{bmatrix}, \tag{30}$$

$$B = \begin{bmatrix} 0 & 1 \end{bmatrix}^T ,$$

where $A_k = \sum_{i=1}^{2} A_k^i s_k^i$. Note that the input matrix is time-invariant for this example, which does not necessarily have to be for the proposed solution methodology. The numerical values for the parameters used for this example are listed in Table 1.

Table 1. Numerical values of the parameters for example 1.

| N	ω_0	β_1	β_2	ζ_1	ζ_2
50	4π	0.1	0.2	0.3	0.1

Now, the true values of the Fourier series coefficients for A_k^1 and A_k^2 can be computed as

$$\mathcal{A}_0^1 = \begin{bmatrix} 0.0000 & 1.0000 \\ 0.0300 & 0.0300 \end{bmatrix}, \mathcal{A}_1^1 = \begin{bmatrix} 0.0000 & 0.0000 \\ 0.0500 & j0.0500 \end{bmatrix}, \mathcal{B}_0^1 = \begin{bmatrix} 0.0000 \\ 1.0000 \end{bmatrix},$$

$$\mathcal{A}_0^2 = \begin{bmatrix} 0.0000 & 1.0000 \\ 0.0200 & 0.0200 \end{bmatrix}, \mathcal{A}_1^2 = \begin{bmatrix} 0.0000 & 0.0000 \\ 0.1000 & j0.1000 \end{bmatrix}, \mathcal{B}_0^2 = \begin{bmatrix} 0.0000 \\ 1.0000 \end{bmatrix}, \tag{31}$$

where $\mathcal{A}_1^1 = (\mathcal{A}_{-1}^1)^*$ and $\mathcal{A}_1^2 = (\mathcal{A}_{-1}^2)^*$.

Having defined the example problem, we now simulate the system to collect the necessary input–output data for the system identification process. To accomplish this, we simulated the difference equation given in Eq. (28) with single frequency cosine and sine input signals in the forms $u_k = \cos(\alpha\omega_0 k)$ and $u_k = \sin(\alpha\omega_0 k)$, respectively. In total, we performed 50 simulation tests (25 cosines and 25 sines) for $\alpha = 0, 1, \ldots, 24$. Each input signal was 1000 samples long corresponding to 10 s in terms of numerical system parameters.

We then apply the proposed system identification methodology to estimate the Fourier series coefficients. At this step, we first need to choose H defined in Eq. (25) to constrain the number of Fourier series coefficients to be estimated. Note that choosing an H value lower than the harmonics of the actual system will result in an oversimplified system, which may not capture the harmonic responses of the original behavior. In contrast, choosing an H value larger than the number of harmonics should result in insignificant magnitudes for higher
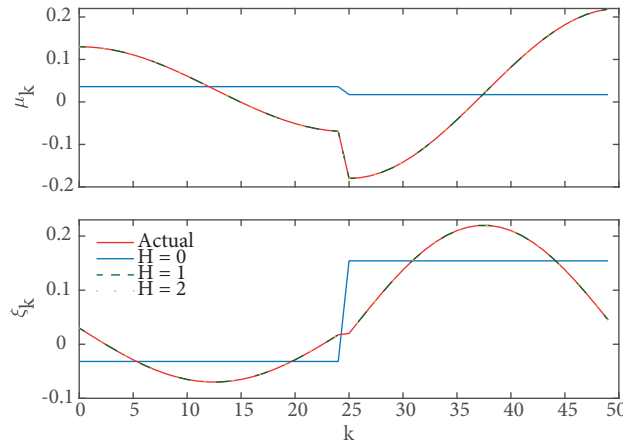
Figure 2. Estimation results for compliance μ_k and damping ξ_k for a single period using $H = 0$, $H = 1$, and $H = 2$ harmonics.

order harmonics, which was not captured in the original system behavior. Hence, choosing a relatively larger H value should not bring any major disadvantage except increasing the computational complexity of the solutions.

The estimated Fourier series coefficients of Eq. (28) for $H = 1$ are computed as

$$
\hat{\mathcal{A}}_0^1 = \begin{bmatrix} 0.0000 & 1.0000 \\ 0.0300 & 0.0300 \end{bmatrix}, \hat{\mathcal{A}}_1^1 = \begin{bmatrix} 0.0000 & 0.0000 \\ 0.0500 & j0.0500 \end{bmatrix}, \hat{\mathcal{B}}_0^1 = \begin{bmatrix} 0.0000 \\ 1.0000 \end{bmatrix},
$$
$$
\hat{\mathcal{A}}_0^2 = \begin{bmatrix} 0.0000 & 1.0000 \\ 0.0200 & 0.0200 \end{bmatrix}, \hat{\mathcal{A}}_1^2 = \begin{bmatrix} 0.0000 & 0.0000 \\ 0.1000 & j0.1000 \end{bmatrix}, \hat{\mathcal{B}}_0^2 = \begin{bmatrix} 0.0000 \\ 1.0000 \end{bmatrix}.
$$

(32)

Note that the proposed method accurately estimates the original Fourier series coefficients as expected by the derivation of the solution methodology. Ensuring that the necessary frequency range is covered by the input signal (entire band is covered in our case) and a sufficient number of harmonics are included, the proposed method should estimate the original parameters accurately. However, if the user considers a lower number of harmonics during the system identification process, some key features of the system may not appear in the output and hence system identification performance might be degraded drastically. To investigate this, we choose $H = 0$ for the same example, where we only consider the responses at the given frequency (as an LTI system). In this case, the estimated Fourier series coefficients become

$$
\hat{\mathcal{A}}_0^1 = \begin{bmatrix} 0.0000 & 1.0000 \\ 0.0196 & 0.0027 \end{bmatrix}, \qquad \hat{\mathcal{B}}_0^1 = \begin{bmatrix} 0.0000 \\ 0.9765 \end{bmatrix},
$$
$$
\hat{\mathcal{A}}_0^2 = \begin{bmatrix} 0.0000 & 1.0000 \\ -0.0676 & 0.2810 \end{bmatrix}, \qquad \hat{\mathcal{B}}_0^2 = \begin{bmatrix} 0.0000 \\ 0.8979 \end{bmatrix}.
$$

(33)

Note that the estimated Fourier series coefficients are very erroneous in this case. However, on the other hand, choosing $H = 2$ yields the same estimates as Eq. (32) for $\hat{\mathcal{A}}_0^1$, $\hat{\mathcal{A}}_1^1$, $\hat{\mathcal{A}}_0^2$, and $\hat{\mathcal{A}}_1^2$. $\hat{\mathcal{A}}_0^3$ and $\hat{\mathcal{A}}_1^3$ have magnitudes in the order of 10^{-16} and are considered to be 0 in our solutions.

In order to present a comparative result of different selections for H, we computed the estimates for μ_k and ξ_k as illustrated in Figure 2. Note that the actual values for the compliance and damping terms have a hybrid nature, where their values switch at the beginning and at half of the system period. It is also important

to note that each switching component also has a time-periodic nature. The estimations with $H = 1$ yield accurate predictions for both μ_k and ξ_k. However, when $H = 0$, the proposed method only estimates the DC terms without any harmonics with a very poor prediction performance. On the other hand, when $H = 2$, the estimation performance is still very accurate although the computational complexity of the solutions increases. This result suggests that choosing a sufficiently large number of harmonics is crucial in order to obtain accurate system identification results.

A simple approach therefore would be starting the identification process with a sufficiently large number. One can utilize the frequency response characteristics of the LTP system to single frequency sinusoidal inputs to make this choice. As noted earlier, a sinusoidal input at ω_c results in harmonic responses at $\omega_c \pm k\omega_0$ for $k \in \mathbf{Z}$. One can perform a frequency sweep across the range of interest for system identification and find the maximum number of harmonics observed as potential candidates for H. Next, if parsimonious models are required, one might reduce H to test for reduced order solutions by comparing the estimation performance with the initial estimation of H. One may also prefer to use statistical analysis techniques, such as the Akaike information criterion (AIC) [32], to decide on the number of harmonics that will be used during the system identification process. This type of analysis deserves and requires an in-depth investigation and is left out of the scope of the current paper.

Finally, we contaminated the system identification data by adding zero-mean white Gaussian noise to our output measurements following the technique used in [9]. This will allow us to test the efficiency of the proposed algorithm in a more realistic simulation setting. Figure 3 illustrates the estimation of performance of the proposed algorithm under different noise contamination levels. Note that the addition of noise deteriorates the prediction performance. The prediction performance of the algorithm is robust to noise up to a signal-to-noise (SNR) ratio of 30 with minimal effect. The prediction error goes up to 6%–7% for some k values when SNR is 20 (note the scale difference between the vertical axes). We also quantified the overall percentage prediction error for the system matrices given in Eq. (31). To achieve this, we concatenated the actual system matrices in Eq. (31) in a single matrix, $\mathcal{A}^{act}$. Similarly, we concatenated the estimated system matrices of Eq. (32) in a single matrix, $\mathcal{A}^{est}$. The percentage prediction error is defined as

$$E_p =: 100 \frac{|\mathcal{A}^{act} - \mathcal{A}^{est}|_2}{|\mathcal{A}^{act}|_2}. \tag{34}$$

The percentage prediction errors for different SNR values are given in Table 2. Our results show that the overall prediction performance of the proposed algorithm remains robust to noise contamination.

Table 2. Percentage prediction error under different noise realizations.

SNR	∞	40	30	20
E_p	10^{-11}	0.234	0.940	2.50

5. Conclusions

A substantial amount of dynamical systems in nature and engineering exhibit rhythmic and quasiperiodic behaviors and hybrid characteristics [6, 10, 33–36]. Analysis and identification of such systems is very critical for scientific and engineering communities. There exist some recent studies that addressed the system identification of rhythmic and periodic dynamical systems [19, 37–39]. Ankarali and Cowan [12] showed that rhythmic hybrid
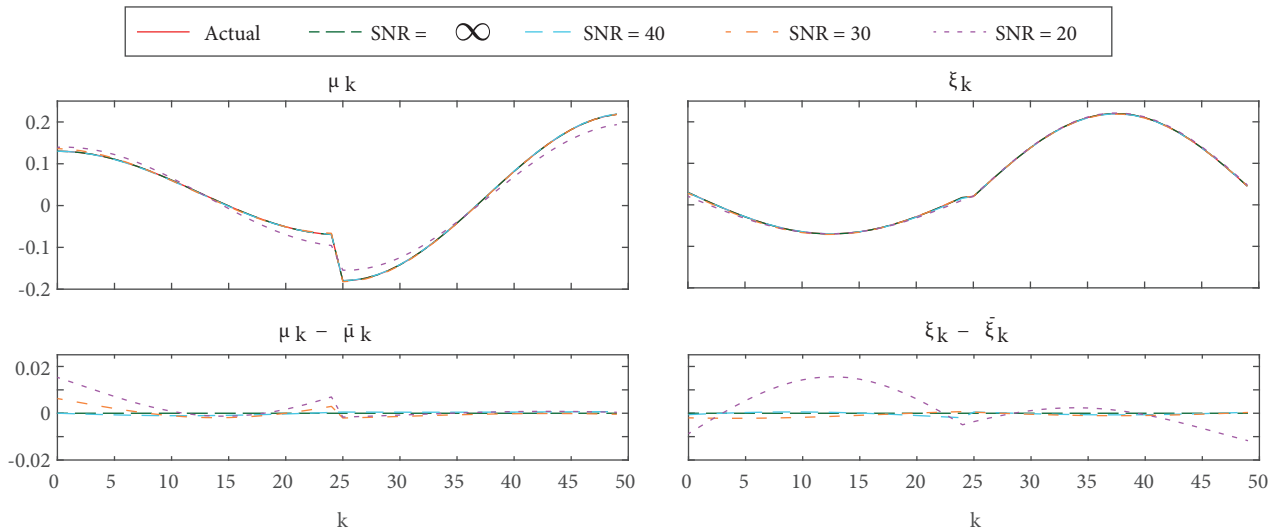
Figure 3. Estimation results for compliance μ_k and damping ξ_k for a single period using $H = 1$ harmonics under different noise realizations.

dynamical systems that have an isolated stable limit cycle can be locally approximated as a (switching) LDTP system by choosing a set of appropriate Poincaré sections. They later proposed a nonparametric frequency-domain system identification approach to LDTP systems. Technically, this study illustrated that switching-based LDTP formulation has very wide application in the dynamical systems community.

In this context, our focus is on developing a parametric frequency-domain system identification method for "hybrid" or switching LDTP systems. The LDTP systems that we focus on in this paper comprise some periodic scheduling signals, which triggers the switching between the individual LDTP subsystems. In our approach, we first collect input–output data from the systems, where inputs are chosen to be sinusoidal signals due to the frequency domain nature of the method. We later put the identification problem in a linear regression framework by considering the Fourier series coefficients of time-periodic input–output data (at steady-state), periodic scheduling signals, and time-periodic system and input matrices. We later estimate the Fourier series coefficients of the time-periodic system and input matrices (which are the unknowns in our formulation) using a least-squares solution. One should also note the fact that in some problems we may already "know" some of the parameters prior from the identification. For example, it is possible that the state-space structure of some of the subsystems can be accurately computed or measured using white-box or gray modeling techniques. Due to the linear regression framework, it would be rather easy to incorporate known parameters and coefficients, which also strengthens the feasibility of our approach.

Finally, we performed a simulation experiment in order to test the feasibility and accuracy of our method using a simulated switching piecewise smooth LDTP system. We successfully showed that if the assumed number of harmonics is larger than or equal to the maximum number of harmonics that the sub-systems cover, we can estimate system parameters and coefficients accurately in a deterministic scenario. We also showed that in a scenario where the number of harmonics is underestimated, the identification results may suffer greatly from underfitting. It is surely possible that in a stochastic setting overfitting may be inevitable if the number of harmonics is overestimated. In the future, we are planning to investigate the performance of our method under noisy conditions (measurement and process), as well as develop a method for choosing the number of harmonics by adopting a statistical model selection framework, e.g., AIC, BIC, or cross-validation.

References

[1] Zhai G, Hu B, Yasuda K, Michel AN. Qualitative analysis of discrete-time switched systems. In: Proceedings of the American Control Conference, Vol. 3; Anchorage, AK, USA; 2002. pp. 1880-1885.

[2] van Wingerden JW, Felici F, Verhaegen M. Subspace identification of MIMO LPV systems using a piecewise constant scheduling sequence with hard/soft switching. In: Proceedings of the European Control Conference; Kos, Greece; 2007. pp. 927-934.

[3] Lin H, Antsaklis PJ. Stability and stabilizability of switched linear systems: a survey of recent results. IEEE Transactions on Automatic Control 2009; 54 (2): 308-322.

[4] Uyanik I, Saranli U, Morgül Ö, Ankarali MM. Parametric identification of hybrid linear time-periodic systems. IFAC-PapersOnLine 2016; 49 (9): 7-12.

[5] DaCunha JJ, Davis JM. A unified Floquet theory for discrete, continuous, and hybrid periodic linear systems. Journal of Differential Equations 2011; 251 (11): 2987-3027.

[6] Holmes P, Full RJ, Koditschek D, Guckenheimer J. The dynamics of legged locomotion: models, analyses, and challenges. SIAM Review 2006; 48 (2): 207-304.

[7] Verdult V, Verhaegen M. Subspace identification of piecewise linear systems. In: Proceedings of the IEEE International Conference on Decision and Control, Vol. 4; Paradise Island, Bahamas; 2004. pp. 3838-3843.

[8] Seipel J, Holmes P. A simple model for clock-actuated legged locomotion. Regular and Chaotic Dynamics 2007; 12 (5): 502-520.

[9] Hwang S. Frequency domain system identification of helicopter rotor dynamics incorporating models with time periodic coefficients. PhD, University of Maryland, College Park, MD, USA, 1997.

[10] Mollerstedt E, Bernhardsson B. Out of control because of harmonics-an analysis of the harmonic response of an inverter locomotive. IEEE Control Systems 2000; 20 (4): 70-81.

[11] Allen MS, Sracic MW, Chauhan S, Hansen MH. Output-only modal analysis of linear time-periodic systems with application to wind turbine simulation data. Mechanical Systems and Signal Processing 2011; 25 (4): 1174-1191.

[12] Ankarali MM, Cowan NJ. System identification of rhythmic hybrid dynamical systems via discrete time harmonic transfer functions. In: Proceedings of the IEEE International Conference on Decision and Control; Los Angeles, CA, USA; 2014. pp. 1017-1022.

[13] Hiskens IA, Reddy PB. Switching-induced stable limit cycles. Nonlinear Dynamics 2007; 50 (3): 575-585.

[14] Uyanik I, Ankarali MM, Cowan NJ, Morgül Ö, Saranli U. Toward data-driven models of legged locomotion using harmonic transfer functions. In: Proceedings of the IEEE International Conference on Advanced Robotics; İstanbul, Turkey; 2015. pp. 357-362.

[15] Hamzacebi H, Morgül Ö. On the periodic gait stability of a multi-actuated spring-mass hopper model via partial feedback linearization. Nonlinear Dynamics 2017; 88: 1237–1256.

[16] Sracic MW, Allen MS. Method for identifying models of nonlinear systems using linear time periodic approximations. Mechanical Systems and Signal Processing 2011; 25 (7): 2705-2721.

[17] Uyanik I. Identification of legged locomotion via model-based and data-driven approaches. PhD, Bilkent University, Ankara, Turkey, 2017.

[18] Bittanti S, Colaneri P. Invariant representations of discrete-time periodic systems. Automatica 2000; 36 (12): 1777-1793.

[19] Uyanik I, Saranli U, Ankarali MM, Cowan NJ, Morgul O. Frequency-domain subspace identification of linear time periodic (LTP) systems. IEEE Transactions on Automatic Control 2019; 64: 2529-2536.

[20] Verhaegen M, Yu X. A class of subspace model identification algorithms to identify periodically and arbitrarily time-varying systems. Automatica 1995; 31 (2): 201-216.

[21] Goos J, Lataire J, Pintelon R. Estimation of affine LPV state space models in the frequency domain: extension to transient behavior and non-periodic inputs. In: Proceedings of the IEEE European Control Conference; Linz, Austria; 2015. pp. 824-829.

[22] Van Wingerden JW, Verhaegen M. Subspace identification of bilinear and LPV systems for open-and closed-loop data. Automatica 2009; 45 (2): 372-381.

[23] Van Overschee P, De Moor B. Subspace Identification for Linear Systems: Theory, Implementation, Applications. Dordrecht, the Netherlands: Springer, 2012.

[24] Katayama T. Subspace Methods for System Identification. Dordrecht, the Netherlands: Springer, 2006.

[25] Di Ruscio D. Subspace System Identification: Theory and Applications. Lecture Notes. Porsgrunn, Norway: Telemark University College, 1997.

[26] Orfanidis SJ. Introduction to Signal Processing. Upper Saddle River, NJ, USA: Prentice-Hall, Inc., 1995.

[27] Uyanik I, Ankarali MM, Cowan NJ, Saranli U, Morgül Ö. Identification of a vertical hopping robot model via harmonic transfer functions. Transactions of the Institute of Measurement and Control 2016; 38 (5): 501-511.

[28] Allievi A, Soudack A. Ship stability via the Mathieu equation. International Journal of Control 1990; 51 (1): 139-167.

[29] Mathews J, Walker RL. Mathematical Methods of Physics. Vol. 501. Menlo Park, CA, USA: WA Benjamin, 1970.

[30] Humphries S. Principles of Charged Particle Acceleration. Mineola, NY, USA: Dover Publications, Inc., 2013.

[31] Ruby L. Applications of the Mathieu equation. American Journal of Physics 1996; 64 (1): 39-44.

[32] Akaike H. A new look at the statistical model identification. IEEE Transactions on Automatic Control 1974; 19 (6): 716-723.

[33] Hausdorff JM. Gait dynamics, fractals and falls: finding meaning in the stride-to-stride fluctuations of human walking. Human Movement Science 2007; 26 (4): 555-589.

[34] Tytell ED, Hsu CY, Williams TL, Cohen AH, Fauci LJ. Interactions between internal forces, body stiffness, and fluid environment in a neuromechanical model of lamprey swimming. Proceedings of the National Academy of Sciences of the USA 2010; 107 (46): 19832-19837.

[35] Dickinson MH, Farley CT, Full RJ, Koehl M, Kram R et al. How animals move: an integrative view. Science 2000; 288 (5463): 100-106.

[36] Grizzle JW, Abba G, Plestan F. Asymptotically stable walking for biped robots: analysis via systems with impulse effects. IEEE Transactions on Automatic Control 2001; 46 (1): 51-64.

[37] Louarroudi E, Pintelon R, Lataire J. Nonparametric tracking of the time-varying dynamics of weakly nonlinear periodically time-varying systems using periodic inputs. IEEE Transactions on Instrumentation and Measurement 2012; 61 (5): 1384-1394.

[38] Logan D, Kiemel T, Jeka JJ. Using a system identification approach to investigate subtask control during human locomotion. Frontiers in Computational Neuroscience 2016; 10: 146.

[39] Burden S, Ohlsson H, Sastry SS. Parameter identification near periodic orbits of hybrid dynamical systems. In: Proceedings of the IFAC Symposium on System Identification; Brussels, Belgium; 2012. pp. 1197-1202.